2011

Catalytic conversion of biomass-derived feedstocks into olefins and aromatics with ZSM-5: the hydrogen to carbon effective ratio

George W Huber, *University of Massachusetts - Amherst*
H. Zhang
Y. Cheng
T. P Vispute
R. Xiao

PAPER

Catalytic conversion of biomass-derived feedstocks into olefins and aromatics with ZSM-5: the hydrogen to carbon effective ratio

Huiyan Zhang,[ab] Yu-Ting Cheng,[b] Tushar P. Vispute,[b] Rui Xiao[a] and George W. Huber[*b]

Catalytic conversion of ten biomass-derived feedstocks, *i.e.* glucose, sorbitol, glycerol, tetrahydrofuran, methanol and different hydrogenated bio-oil fractions, with different hydrogen to carbon effective (H/C_{eff}) ratios was conducted in a gas-phase flow fixed-bed reactor with a ZSM-5 catalyst. The aromatic + olefin yield increases and the coke yield decreases with increasing H/C_{eff} ratio of the feed. There is an inflection point at a H/C_{eff} ratio = 1.2, where the aromatic + olefin yield does not increase as rapidly as it does prior to this point. The ratio of olefins to aromatics also increases with increasing H/C_{eff} ratio. CO and CO_2 yields go through a maximum with increasing H/C_{eff} ratio. The deactivation rate of the catalyst decreases significantly with increasing H/C_{eff} ratio. Coke was formed from both homogeneous and heterogeneous reactions. Thermogravimetric analysis (TGA) for the ten feedstocks showed that the formation of coke from homogeneous reactions decreases with increasing H/C_{eff} ratio. Feedstocks with a H/C_{eff} ratio less than 0.15 produce large amounts of undesired coke (more than 12 wt %) from homogeneous decomposition reactions. This paper shows that the conversion of biomass-derived feedstocks into aromatics and olefins using zeolite catalysts can be explained by the H/C_{eff} ratio of the feed.

1. Introduction

Production of high-grade liquid fuels and chemicals from lignocellulosic biomass is one of the most promising ways to solve energy and environmental problems caused by our dependence on fossil oil.[1,2] Zeolite catalysts are the workhorse of the petroleum industry efficiently converting petroleum-based feedstocks into targeted fuels and chemicals.[3–6] Zeolite catalysts have also been shown to be promising for conversion of biomass-derived feedstocks into fuels and chemicals.[7–14] The main

challenge for biomass and its derived feedstocks catalytic conversion is how to improve catalyst properties and process conditions to obtain high yields of hydrocarbons while minimizing coke formation on the zeolites.[15] Over the last twenty years, there have been dozens of studies that focused on the catalytic conversion of biomass and its derived feedstocks with a range of zeolite catalysts including ZSM-5, Beta, Y, mordenite, FCC, Al-MCM-41, SBA-15, Al-MSU-F FER, MFI and MOR.[16–44] Furthermore, the designs and applications of zeolite catalysts for biomass conversion have also been well reviewed.[45–50] In these zeolite catalysts, ZSM-5 has shown the highest aromatic and olefin yields from lignocellulosic biomass.[43,44] ZSM-5 has a 3-dimensional pore system with a pore size of 5.5–5.6 Å based on atomic radii.[44] The small pore size, internal structure and internal volume make it difficult for larger

[a]School of Energy and Environment, Southeast University, Nanjing, 210096, PR China
[b]Department of Chemical Engineering, University of Massachusetts-Amherst, Amherst, MA, 01002, USA. E-mail: huber@ecs.umass.edu; Tel: +1 4135450276

Broader context

Catalytic fast pyrolysis (CFP) is a promising technology to directly convert solid biomass into gasoline-range aromatics over zeolite catalysts. During CFP, biomass-derived feedstocks undergo a hydrocarbon pool mechanism occurring within the zeolite framework. The lifetime and product distribution of the hydrocarbon pool varies with different biomass-derived feedstocks. In this study we show that the product distribution from catalytic fast pyrolysis of biomass-derived feedstocks is a function of the hydrogen to carbon effective ratio (H/C_{eff}) of the feed. Upgraded bio-oils with higher H/C_{eff} ratios give more valuable products (olefins + aromatics) and less coke than those without upgrading. We suggest a H/C_{eff} value for upgrading biomass-derived feedstocks to optimize valuable products yield in the following CFP process. We also show how the catalyst activity changes with feedstocks that have different H/C_{eff} ratios.

This journal is © The Royal Society of Chemistry 2011

Energy Environ. Sci., 2011, **4**, 2297–2307 | 2297

aromatic coke precursors to form inside of the pores.[9,44] Several reactions occur inside the zeolite including dehydration, decarboxylation, isomerization and decarbonylation thereby removing oxygen as water, carbon monoxide and carbon dioxide and converting the carbon and hydrogen into olefins and aromatics.[31]

The main problem for biomass conversion with zeolites is that the biomass-derived feedstocks typically produce large amount of coke, a wide variety of products are produced, and the zeolite catalyst is deactivated rapidly.[11,51,52] Chen et al.[52] introduced the hydrogen to carbon effective (H/C$_{eff}$) ratio, as shown in eqn (1), to describe whether a feed can be economically converted into hydrocarbons using zeolite catalyst according to the amount of oxygen, carbon, and hydrogen in the feed. The H, C and O in eqn (1) are the moles of hydrogen, carbon, and oxygen in the feed, respectively.

$$H/C_{eff} = \frac{H - 2O}{C} \quad (1)$$

Chen et al.[52] stated that feedstocks with H/C$_{eff}$ ratios less than 1 are difficult to upgrade to produce premium products over a ZSM-5 catalyst due to rapid aging and deactivation of the catalyst. The H/C$_{eff}$ ratio of petroleum-derived feedstocks is between 1 and 2. The H/C$_{eff}$ ratio of lignocellulosic biomass is between 0 and 0.3. Therefore, biomass is made of hydrogen-deficient molecules, and strategies for biomass and its derived feedstocks conversion must take their H/C$_{eff}$ ratio into account.

Fig. 1 shows the reaction schematic of biomass-derived feedstocks over the ZSM-5 catalyst. Feedstocks with different H/C$_{eff}$ ratios first undergo dehydration and decarbonylation reactions to make intermediate oxygenates as well as CO, CO$_2$, H$_2$O and homogeneous coke as by-products on the surface of the catalyst. Then these intermediate oxygenates diffuse into the zeolite catalyst pores and form aromatics and olefins as well as heterogeneous coke through a series of decarbonylation, decarboxylation, dehydration, and oligomerization reactions. The oxygen in the feedstocks is removed in the form of CO, CO$_2$ and H$_2$O. It has been reported that the aromatics formation reaction undergoes through a common intermediate or a "hydrocarbon pool" within the zeolite framework.[53–59]

Recently, we outlined a new method for bio-oil upgrading where hydroprocessing of bio-oils with Ru/C and Pt/C catalysts followed by conversion with zeolite catalysts was able to produce aromatics and olefins in yields 2 to 3 times higher than zeolite conversion of the bio-oils without hydrogenation.[60] The purpose

of the hydroprocessing was to add hydrogen selectively to the biomass-derived feedstocks thereby increasing the H/C$_{eff}$ ratio of the feed. We also tested the zeolite conversion of other feedstocks and showed that the aromatic + olefin yield increased with an increasing H/C$_{eff}$ ratio of the feed. The purpose of this paper is to explain more in depth how the product selectivity and catalyst activity change for ten different biomass-derived feedstocks over a ZSM-5 catalyst. Thermogravimetric analysis (TGA) was used to obtain the homogeneous coke yield of all the feedstocks. The deactivation rates of the ZSM-5 catalyst were calculated. Furthermore, the formations of homogeneous and heterogeneous coke were discussed as well as how the product selectivity changes with different feedstocks.

2. Experimental section

2.1. Materials

2.1.1. Biomass-derived feedstocks. Ten biomass-derived feedstocks with different H/C$_{eff}$ ratio were converted, including pure compound solutions and bio-oil derived feedstocks. Pure compound solutions, including glucose, sorbitol, glycerol, tetrahydrofuran (THF) and methanol, were dissolved and/or mixed in water with a mass percentage of 12.5 wt%. The bio-oil derived feeds were made from DOE bio-oil (DOE-BO) and pine wood bio-oil (PWBO), including DOE-BO, low-temperature hydrogenated DOE bio-oil (LTH-DOE-BO), water-soluble bio-oil of pine wood (WSBO), low temperature hydrogenated water-soluble bio-oil (LTH-WSBO) and high temperature hydrogenated water-soluble bio-oil (HTH-WSBO). DOE-BO was supplied by the US Department of Energy (DOE) and was manufactured by the National Renewable Energy Laboratory (NREL) from white oak pellets using the Thermochemical Process Development Unit (TCPDU). PWBO was obtained from the Mississippi State University and was produced by pyrolysis of dry pine wood in an auger reactor. LTH-DOE-BO was obtained by low temperature hydrogenation of DOE-BO with 5 wt% Ru/C catalyst at a temperature of 125 °C, pressure of 100 bar and WHSV of 1.6 h^{-1}. The WSBO was prepared by mixing 7 g PWBO with 28 g water and decanting the top layer. Detailed information about how the hydrogenated bio-oils were produced can be found in our previous work.[60] In brief summary, LTH-WSBO was produced by hydrogenation of WSBO with 5 wt% Ru/C catalyst at a temperature of 125 °C, pressure of 52 bar and WHSV of 3 h^{-1}. HTH-WSBO was produced from two-stage hydrogenation of WSBO. The first stage was operated with 5 wt% Ru/C catalyst at a temperature of 125 °C, pressure of 100 bar and WHSV of 3 h^{-1}. The second stage was operated with 5 wt% Pt/C catalyst at a temperature of 250 °C, pressure of 100 bar and WHSV of 3 h^{-1}. The distributions of the products identified in the bio-oil fractions are listed in Table 1. In the WSBO fraction over 55% of the carbon was identified. The remaining carbon was probably present as carbohydrate oligomers that were not detected by our methods. Only about one-third of the products can be identified in DOE-BO and LTH-DOE-BO. The pure bio-oil fractions contained large amounts of polymeric lignin oligomers which had a M_w from 300 to 7000 daltons (Da). Compared to DOE-BO, the LTH-DOE-BO has a higher concentration of oligomers with a molecular weight greater than 400 Da.
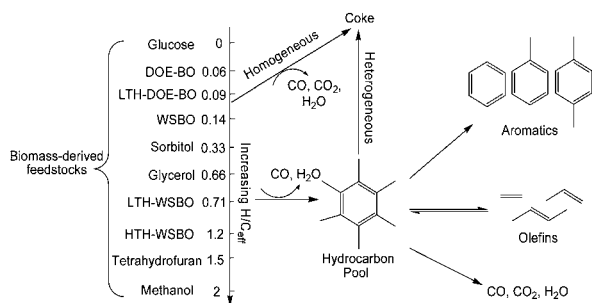

Fig. 1 Reaction schematic of biomass-derived feedstocks with ZSM-5 catalyst.

Table 1 Carbon product selectivity (%) of the bio-oil feedstocks (for DOE-BO and LTH-DOE-BO, based on elemental analysis; for WSBO, LTH-WSBO and HTH-WSBO, based on the total carbon measured by TOC)

Compound	DOE-BO	LTH-DOE-BO	WSBO	LTH-WSBO	HTH-WSBO
Acetic acid	8.42	10.01	6.29	5.66	3.08
Methyl acetate	0.13	0.25			
Hydroxyacetone	1.63	2.17	5.14		
2-Furanone	0.50	0.40	0.97		
3-Methyl-1,2-cyclopentadione	0.44		1.18		
1-Hydroxy-2-butanone	0.52	0.52			
2-Cyclopenten-1-one	0.31		0.56		
Hydroxyacetaldehyde	8.96		11.02		
Furfural	0.63	0.44	0.54		
5-Hydroxymethylfurfural	0.64		1.65		
Phenol	0.11	0.35	0.06		
γ-Butyrolactone	0.22			2.87	3.25
γ-Valerolactone				0.27	0.37
4-Hydroxymethyl-γ-butyrolactone				1.95	1.38
Tetrahydrofuran					0.18
2-Methyltetrahydrofuran					0.63
2,5-Dimethyltetrahydrofuran					0.58
Methanol	0.27	0.27	0.63	1.37	1.67
Ethanol				0.55	1.41
1-Propanol				0.27	1.25
1-Butanol				0.12	0.34
2-Butanol					0.44
1-Pentanol					0.25
2-Pentanol					0.13
Ethylene glycol				13.87	13.66
Cyclopentanol				0.26	0.68
2-Hexanol					0.23
Propylene glycol				5.11	9.32
2,3-Butanediol					1.02
Cyclohexanol				3.47	1.51
1,2-Butanediol				0.89	4.03
Tetrahydrofurfuryl alcohol				0.03	2.13
1,4-Butanediol				1.51	2.01
Glycerol					1.43
1,2-Cyclohexanediol				2.98	3.16
Sorbitol		0.17		10.78	0.64
Guaiacol			0.27		
Catechol			6.44		
4-Methyl catechol			1.22		
3-Methylcyclopentanol					1.00
1,2,3-Butanetriol					0.86
1,4-Pentanediol					0.68
3-Methylcyclohexanol					1.01
4-Methylcyclohexanol					0.60
1,2-Hexanediol					0.81
1,2,6-Hexanetriol					0.42
Levoglucosan	8.73	7.48	16.82	9.52	
Sugars	1.75	1.36	3.21	1.20	0.19
Total carbon identified	33.26	22.9	56.52	62.68	60.35
Unidentified carbon	66.74	77.1	43.48	37.32	39.65

2.1.2. Catalyst. A ZSM-5 catalyst (CBV 3024E, $SiO_2/Al_2O_3 = 30$) obtained from Zeolyst was used for all of these studies. The catalyst was sieved to a particle size of 425–800 μm before being placed into the reactor (described below). The catalyst was calcined in the reactor at a temperature of 600 °C with 60 mL min^{-1} air (Airgas, regular-high purity, dehumidified by a drierite tube) for 6 hours prior to reactions.

2.2. Experimental setup

2.2.1. Gas-phase flow fixed-bed reactor. A gas-phase flow fixed-bed reactor system was built for catalytic conversion of biomass-derived feedstocks into olefins and aromatics as shown in Fig. 2. This reactor consists of a gas feed system, a liquid feeding unit, the reactor, the heater for the reactor, a condensor and a gas sample collecting unit. A quartz tube of 12.5 mm OD was used as the reactor. Sieved ZSM-5 powders were held in the reactor by quartz beads (250–425 μm) and quartz wool. The reaction temperature was measured *via* a K-type thermocouple inserted into an inner tube at the top of the catalyst bed. Prior to reactions, the catalyst was calcined as described in Section 2.1.2. Helium was used as a carrier gas (Airgas, 99.999%). The liquid feedstock was introduced into the reactor through a PTFE tube by a syringe pump (Fisher, KDS100). A condenser in an ice-water bath was used to trap heavy products. After reactions, the reactor was flushed by helium with a flow rate of 100 mL min^{-1}
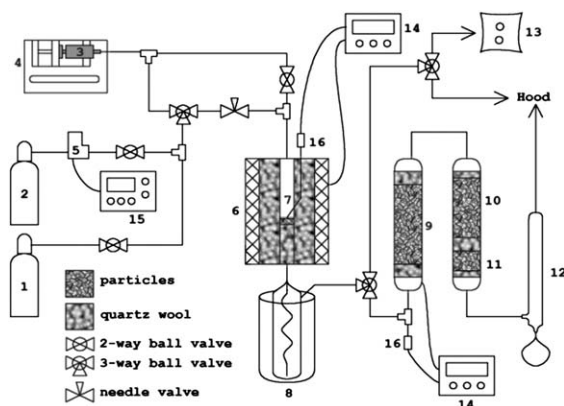
Fig. 2 Schematic diagram of catalytic conversion of biomass-derived feedstocks into olefins and aromatics system. (1) Air cylinder; (2) He cylinder; (3) syringes; (4) syringe pump; (5) mass flow controller; (6) furnace; (7) quartz tubular reactor; (8) ice-water condenser; (9) copper converter; (10) moisture trap (drierite); (11) CO_2 trap (ascarite); (12) bubble flow meter; (13) gas sampling bag; (14) temperature controller; (15) mass flow controlling box; and (16) K-type thermocouple.

for 30 min at the reaction temperature. The condensed products were extracted by adding 10 mL of ethanol into the condenser to obtain liquid products. Gas phase products were collected by an air bag for analysis.

After reaction the carrier gas was switched to air at 60 mL min^{-1} to regenerate the used catalyst. During the regeneration, the produced CO was further converted into CO_2 by using a copper converter catalyst (13 wt% CuO on alumina, Sigma-Aldrich) which was heated to 250 °C. The CO_2 was trapped by a CO_2 trap (Ascarite, Sigma-Aldrich). The coke yield was obtained by measuring the mass change of the CO_2 trap.

Unless otherwise mentioned, the typical reaction conditions for catalytic conversion of biomass-derived feedstocks used in this study were: temperature of 600 °C, a carrier gas flow rate of 204 mL min^{-1}, a weight hourly space velocity (WHSV) of 11.7 h^{-1} and a ZSM-5 mass of 26 mg.

2.2.2. Thermogravimetric analysis (TGA) experiments. Thermogravimetric analysis (TGA) of the ten feedstocks was carried out in a TGA instrument (TA Instrument, SDT Q600). Before the experiment, an alumina pan filled with 15 mg sample was put into the TGA chamber that was continuously purged by helium at 100 mL min^{-1}. The chamber was programmed with the following temperature regime: hold at room temperature for 0.5 min, ramp to 700 °C at 1.5 °C min^{-1} and hold at 700 °C for 30 min.

2.3. Product analysis and data evaluation

2.3.1. Gas product analysis. The gaseous product was analyzed using a Shimadzu 2014 GC system. A Restek Rtx-VMS capillary column (Catalog No. 19915) (with FID detector) was used to quantify aromatic hydrocarbons, while a HAYSEP D packed column from Supelco was used to analyze CO and CO_2 (with TCD detector). Both FID and TCD detectors were maintained at 240 °C. Ultra high purity helium was used as carrier gas. The following temperature ramp was used in this study: hold at 35 °C for 5 min, ramp to 140 °C at 5 °C min^{-1}, ramp to 230 °C at 50 °C min^{-1} and hold at 230 °C for 8.2 min.

2.3.2. Liquid product analysis. Liquid products were identified by GC-MS (Shimadzu-2010) and quantified by GC-FID (Agilent 7890A). Restek Rtx-VMS capillary column (Catalog No. 19915) was used in the GC-MS system. It was operated at a constant flow rate of 1.9 mL min^{-1} with ultra high purity helium as the carrier gas. The injector and detector were both held at 240 °C. The GC oven was programmed with the following temperature regime: hold at 30 °C for 5 min, ramp to 140 °C at 7.5 °C min^{-1}, ramp to 240 °C at 40 °C min^{-1} and hold at 240 °C for 15 min. The GC-FID system also used ultra high purity helium as the carrier gas. The FID detector was maintained at 250 °C. The product separation was carried out in an Agilent capillary column (Catalog No. 19091J-413). The following column temperature regime was used: hold at 40 °C for 5 min, ramp to 250 °C at 20 °C min^{-1}, and hold at 250 °C for 20 min. However, some compounds such as sugars, sugar alcohols and levoglucosan in bio-oil derived feedstocks cannot be detected by GC-MS and GC-FID. In this study, a high-performance liquid chromatography (HPLC, Shimadzu) system was used to analyze these compounds. An RI detector (held at 30 °C) was used in the system to quantify sugars, sugar alcohol and levoglucosan. Bio-Rad's Aminex HPX-87H column (Catalog No. 125-0140) was used with 0.005 M H_2SO_4 as the mobile phase with the flow rate of 1 mL min^{-1}. The column oven temperature was held at 30 °C. The carbon content in WSBO, LTH-WSBO and HTH-WSBO were determined by Total Organic Carbon (TOC) analysis. The carbon contents in DOE-BO and LTH-DOE-BO were determined by elemental analysis.

2.3.3. Data evaluation. The following calculations were used in this paper:

$$\text{WHSV} = \frac{\text{Mass flow rate of feed (g/h)}}{\text{Mass of catalyst (g)}} \quad (2)$$

$$\text{Carbon yield} = \frac{\text{Moles of carbon in a product}}{\text{Moles of carbon fed in}} \times 100\% \quad (3)$$

$$\text{Carbon selectivity} = \frac{\text{Moles of carbon in a product}}{\text{Moles of carbon in identified products}} \times 100\% \quad (4)$$

$$\text{Coke yield in TGA} = \frac{\text{Mass of residue}}{\text{Mass of feed}} \times 100\% \quad (5)$$

$$\text{Deactive rate} = \frac{y_{c,max} - y_{c,19.5}}{y_{c,max} \times (t_{max} - 19.5)} \times 100\% \quad (6)$$

where $y_{c,19.5}$ is the aromatic + olefin carbon yield at 19.5 min, while $y_{c,max}$ and t_{max} are the maximum aromatic + olefin carbon yield and corresponding time, respectively.

3. Results

3.1. Thermal stability of biomass-derived feedstocks

Biomass-derived feedstocks typically have a low thermal stability meaning that they decompose forming coke, H_2O, CO and CO_2 when heated above a certain temperature in the absence of

Table 2 Homogeneous coke yields obtained using a TGA instrument with the temperature programmed from room temperature to 700 °C at 1.5 °C min^{-1}, followed by an isotherm period of 30 min at 700 °C in an ultra high helium atmosphere. (Glucose, sorbitol, glycerol, THF and methanol are water solutions with a concentration of 12.5 wt%; WSBO contains 12.5 wt% oil fraction.)

Feedstock	Glucose	DOE-BO	LTH-DOE-BO	WSBO	Sorbitol	Glycerol	LTH-WSBO	HTH-WSBO	THF	Methanol
H/C_{eff} ratio	0	0.06	0.09	0.14	0.33	0.66	0.71	1.2	1.5	2
Coke yield (wt%)	23.1	19	13.64	12.8	6.14	0.4	2.82	0.24	0	0

oxygen. TGA was used to study the thermal stability of the feedstocks as stated in Section 2.2.2. Table 2 lists the homogeneous coke yields of the different feedstocks. The coke yield decreases with an increasing H/C_{eff} ratio, indicating that the feedstock with lower H/C_{eff} ratio has lower thermal stability. The feeds with a H/C_{eff} of less than 0.2 had high coke yields from 13 to 23 wt%. Only trace amounts of homogeneous coke was formed for feeds with a H/C_{eff} ratio of greater than 0.6.

3.2. Gas-phase product yields for catalytic conversion of various biomass-derived feedstocks

The product yields for the different feedstocks as a function of time on stream are shown in Fig. 3. The products include aromatics, olefins, CO, CO_2 and coke. The product yields first increase with time on stream to a maximum value and then gradually decrease. After the experiment, products continue to desorb from the catalyst surface (see 20 to 25 minutes time on stream in Fig. 3). This may be due to the decomposition of the real catalytic active center, the hydrocarbon pool, inside the zeolite catalyst. In the first step of the reactions, the feedstocks are consumed to form a hydrocarbon pool inside the zeolite. This hydrocarbon pool needs to take some time to build up. The active centers of the hydrocarbon pool then convert the feed into olefins, aromatics, CO and CO_2. Coke also builds up inside the zeolite which causes deactivation of the active centers and the decrease of aromatic and olefin yields. After reactions, the products that are trapped inside the zeolite take some time to diffuse out after reaction. The aromatic and olefin yields with respect to time on stream for tetrahydrofuran (THF) and methanol are different from the other feedstocks. When THF is the feedstock the olefin yield increases and aromatic yield decreases with time on stream. Catalytic conversion of methanol shows completely opposite trends. This indicates that different hydrocarbon pools were involved in the THF and methanol catalytic conversion. This phenomenon has also been shown in other papers for conversion of methanol with zeolite catalysts.[61,62] This suggests that with methanol the formation of aromatics undergoes several steps which take some time to reach steady state. Methanol first forms dimethyl ether (C2) and then C3, C4, C5 to C6. Only C6 compounds can form aromatic compounds.[58] This means the rate of the hydrocarbon pool formation of methanol for producing aromatics is much slower than the other feedstocks, which are at least C4 compounds. During the methanol conversion process, the olefins are built up in the hydrocarbon pools and finally converted into aromatics.

Table 3 shows the detailed product carbon yields for catalytic conversion of the ten feedstocks. The identified carbon in gas products is between 83% and 100% for all feedstocks. The missing carbon is some oxygenated compounds (for bio-oil
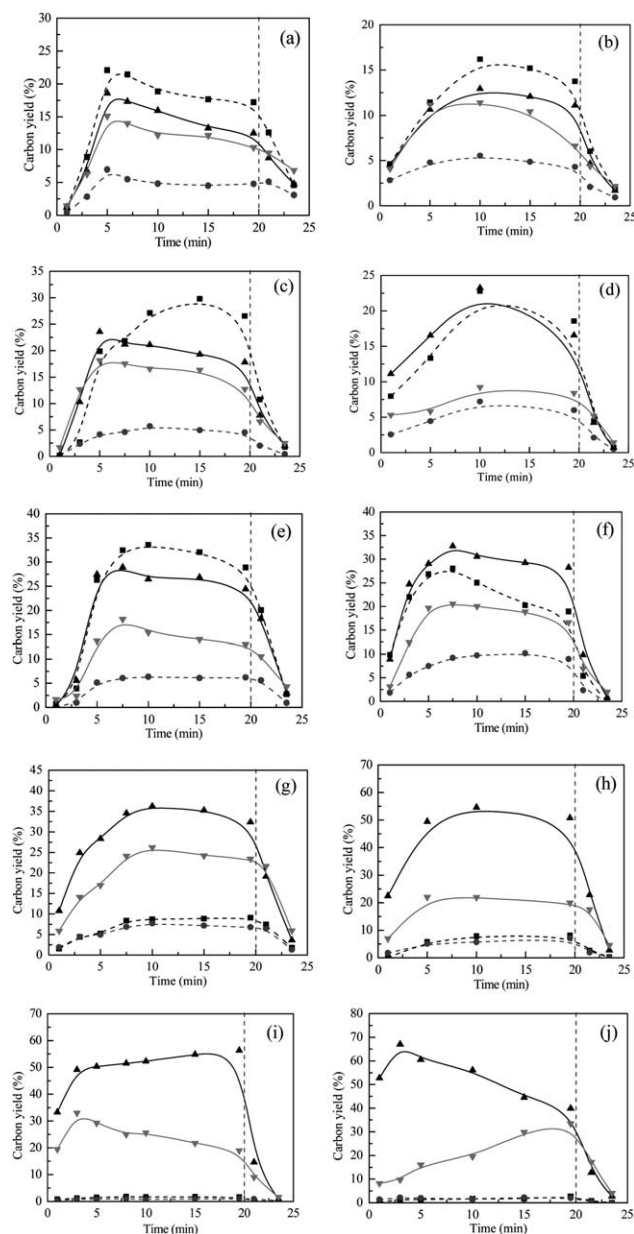

Fig. 3 Product carbon yields as a function of time for catalytic conversion of various biomass-derived feedstocks. (a) 12.5 wt% glucose–water solution; (b) DOE bio-oil; (c) LTH-DOE bio-oil; (d) 12.5 wt% WSBO; (e) 12.5 wt% sorbitol–water solution; (f) 12.5 wt% glycerol–water solution; (g) low temperature hydrogenated WSBO; (h) high temperature hydrogenated WSBO; (i) 12.5 wt% tetrahydrofuran–water solution and (j) 12.5 wt% methanol–water solution. (▲ Olefins; ▼ aromatics; ■ CO; ● CO_2. Yields are based on carbon molar selectivity.)

Table 3 Product carbon yields for catalytic conversion of various biomass-derived feedstocks. (Glucose, sorbitol, glycerol, THF and methanol are water solutions with a concentration of 12.5 wt%; WSBO contains 12.5 wt% oil fraction.)

Feedstock	Glucose	DOE-BO	LTH-DOE-BO	WSBO	Sorbitol	Glycerol	LTH-WSBO	HTH-WSBO	THF	Methanol
H/C_{eff} ratio	0	0.06	0.09	0.14	0.33	0.66	0.71	1.20	1.5	2
Product carbon yields (%)										
CO	18.10	13.49	22.58	17.88	28.30	21.99	8.14	6.82	1.48	1.79
CO_2	5.18	4.80	4.42	5.81	5.75	8.35	6.87	5.71	0.91	2.00
Coke	32.60	49.48	35.29	32.33	14.21	9.35	18.86	14.83	5.71	2.26
Olefins										
Ethylene	5.74	5.79	9.74	7.68	11.01	15.58	10.38	16.27	6.28	23.43
Propylene	6.48	4.06	6.63	8.48	10.51	9.66	18.08	27.27	39.22	23.16
Butylenes	2.08	1.33	2.09	2.31	2.93	2.76	4.24	7.23	5.94	8.93
Sum	14.30	11.18	18.46	18.47	24.45	28.00	32.70	50.77	51.44	55.52
Aromatics										
Benzene	2.85	1.74	2.49	2.17	3.58	3.25	4.08	5.79	8.25	1.37
Toluene	5.14	3.97	5.49	3.80	6.16	8.80	10.56	10.64	11.02	5.23
Xylene	2.78	2.28	5.70	1.70	2.80	4.46	7.34	4.09	4.05	16.53
Ethyl benzene	0.44	0.20	0.50	0.13	0.37	0.38	0.64	0.48	0.42	0.52
Styrene	0.54	0.42	0.37	0.22	0.29	0.38	0.43	0.27	0.28	0.46
Indene	0.34	0.79	0	0.11	0.49	0.51	0.31	0.10	0.37	0.42
Naphthalene	0.23	0.41	0.19	0.06	0.20	0	0	0.10	0.08	0.15
Sum	12.32	9.81	14.74	8.19	13.89	17.78	23.36	21.47	24.47	24.68
Furan	0.63	0.74	1.12	0.63	1.39	0.05	0.81	0.21	0	0
Total carbon yield	83.13	89.5	96.61	83.31	87.99	85.52	90.74	99.81	84.01	86.25

Table 4 Liquid product compositions produced from catalytic conversion of bio-oil derived feedstocks

Compound	Carbon yield (%)				
	WSBO	LTH-WSBO	HTH-WSBO	DOE-BO	LTH-DOE-BO
Phenol	1.26	0.46	0.37	0.02	0.03
3-Methyl-phenol	0.49	0.28	0.18	0	0
2-Methyl-phenol	0.98	0.49	0.31	0.01	0.02
2,6-Dimethyl-phenol	0.28	0.18	0.08	0	0
2,3-Dimethyl-phenol	0.14	0.09	0.03	0	0
4-(2-Furanyl)-3-buten-2-one	0	0.29	0.21	0.09	0.16
2,4-Dimethyl-phenol	0.11	0.07	0.06	0	0
2,3-Dihydro-benzofuran	0.63	0	0	0	0
1-Methyl-naphthalene	0.49	1.15	0	0	0
1-Naphthalenol	0.53	0	0	0	0
2-Naphthalenol	1.26	0.29	0.21	0.08	0.11
Fluorene	0.77	0.42	0.31	0.22	0.48
7-Methyl-1-naphthol	0.95	0	0	0	0
Total yield	7.89	3.72	1.76	0.42	0.8

derived feeds) and C$_5$ hydrocarbons (for methanol) in liquid products (see Table 4 and ref. 63).

3.3. The carbon selectivities of olefin and aromatic products

The olefins produced include: ethylene, propylene and butylenes. The main aromatics detected include: benzene, toluene and xylene. Their selectivities in the products as a function of time on stream can further monitor the change of the hydrocarbon pools with time. Fig. 4 and 5 show the olefin and aromatic selectivities for the ten feedstocks as a function of time on stream, respectively. After the formation of the hydrocarbon pools (>5 min), the selectivities of ethylene and propylene are much higher than those of butylenes for all feeds. For DOE-BO and LTH-DOE-BO, the selectivities of ethylene and butylenes increase with time on stream, whereas for WSBO and glycerol, those of propylene and butylenes increase with time on stream.

For LTH-WSBO and HTH-WSBO, the selectivity of propylene is higher than that of ethylene and is almost the same during the first 20 min.

As shown in Fig. 5, toluene has the highest aromatic selectivity for conversion of all feeds except for methanol. Catalytic conversion of methanol produced xylene in a 70% aromatic selectivity. For catalytic conversion of glucose, DOE-BO, LTH-DOE-BO, WSBO, sorbitol and glycerol (all of them are low H/C_{eff} ratio feedstocks), the aromatic products selectivity shows a significant change with time on stream during the hydrocarbon pool formation phase (the first 5 min of time on stream). After the 5 minutes time on stream formation of the pool, the xylene selectivity decreases and the benzene and toluene selectivities increase for sorbitol, glycerol, LTH-WSBO and HTH-WSBO. The benzene selectivity increases and the toluene selectivity decreases for THF. The aromatic selectivity for methanol has no change after the first 5 min.
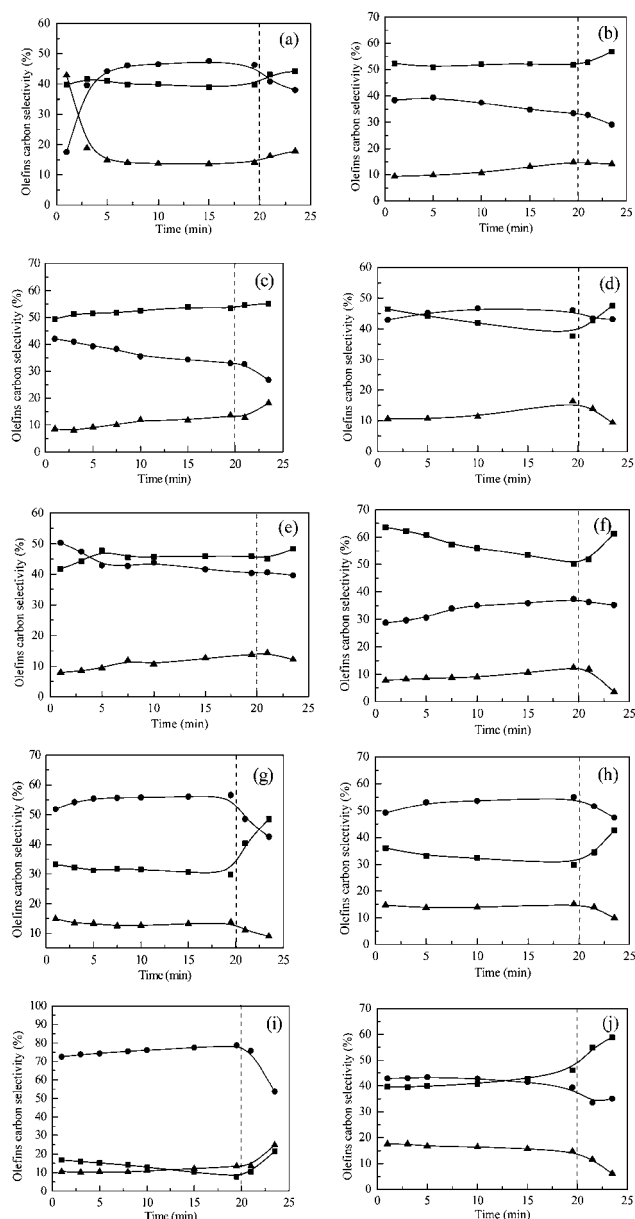
Fig. 4 Olefin product selectivity as a function of time on stream for conversion of: (a) 12.5 wt% glucose–water solution; (b) DOE-BO; (c) LTH-DOE-BO; (d) WSBO; (e) 12.5 wt% sorbitol–water solution; (f) 12.5 wt% glycerol–water solution; (g) LTH-WSBO; (h) HTH-WSBO; (i) 12.5 wt% THF–water solution and (j) 12.5 wt% methanol–water solution. (■ Ethylene; ● propylene; ▲ butylenes. Yields are based on carbon molar selectivity.)

Fig. 5 Aromatic product selectivity as a function of time on stream for conversion of: (a) 12.5 wt% glucose–water solution; (b) DOE-BO; (c) LTH-DOE-BO; (d) WSBO; (e) 12.5 wt% sorbitol–water solution; (f) 12.5 wt% glycerol–water solution; (g) LTH-WSBO; (h) HTH-WSBO; (i) 12.5 wt% THF–water solution and (j) 12.5 wt% methanol–water solution. (■ Benzene; ● toluene; ▲ xylene. Yields are based on carbon molar selectivity.)

3.4. Liquid-phase product yields for catalytic conversion of various bio-oil derived feedstocks

Small amounts of liquid products were also produced for the bio-oil feedstocks. These liquid products contained primarily single-ring phenols, naphthalenols and fluorene as shown in Table 4. The yield of the phenolics decreases in the following order: WSBO > LTH-WSBO > HTH-WSBO > LTH-DOE-BO > DOE-BO. The single-ring phenols in the liquids include phenol, 3-methyl-phenol, 2-methyl-phenol, 2,6-dimethyl-phenol, 2,3-dimethyl-phenol and 2,4-dimethyl-phenol. For WSBO, LTH-
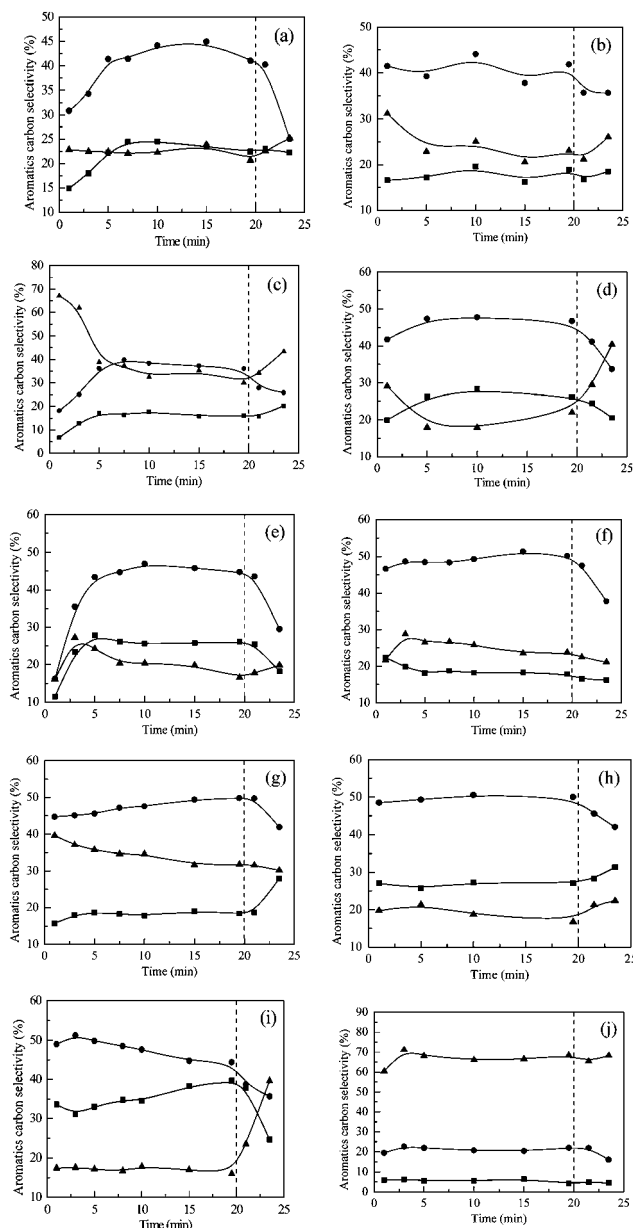
WSBO and HTH-WSBO, the yields of these single-ring phenols are 3.26%, 1.57% and 1.04%, respectively.

4. Discussion

4.1. Product yields as a function of hydrogen to carbon effective (H/C_{eff}) ratio

In zeolite upgrading of an oxygenated hydrocarbon, C6–C8 aromatic hydrocarbons, C2–C4 olefins, CO, and H_2O are the

major products. Oxygen is removed from the feed in the form of CO or H_2O. In this study, the theoretical yield was calculated assuming toluene as the targeted product and CO and H_2O as the byproducts. The overall stoichiometry is shown in eqn (7):

$$C_xH_yO_z \rightarrow aC_7H_8 + bCO + cH_2O \qquad (7)$$

where

$$a = (x + 0.5y - z)/11 \qquad (8)$$

$$b = (4x - 3.5y + 7z)/11 \qquad (9)$$

$$c = (4z + 3.5y - 4x)/11 \qquad (10)$$

When $b < 0$, we assumed H_2 as one of the byproducts instead of CO. Fig. 6 shows the experimental and theoretical aromatic + olefin yield as a function of the H/C_{eff} ratio. The experimental aromatic + olefin yield increases from 27% to 80% with the increase of the H/C_{eff} ratio from 0 (glucose) to 2 (methanol). There is an inflection point at a H/C_{eff} ratio = 1.2, where the aromatic + olefin yield does not increase as rapidly as it does before. This is also the same point where the theoretical yield is 100%. At this point all of the carbon in the feedstock is converted into carbon in the aromatics. This suggests that, if cheap hydrogen is available, the amount of hydrogen that is added to the biomass feedstock should be enough to bring it to a H/C_{eff} ratio of 1.2. Adding more hydrogen to the biomass feedstock would be a waste of hydrogen resources and increase the cost of the process. This also suggests that future biorefineries should target an enrichment of the biomass feedstock to a H/C_{eff} ratio of 1.2.

The experimental/theoretical yield or percentage of the theoretical yield increases with increasing H/C_{eff} ratio as shown in Fig. 6. The theoretical yield of glucose is only 42%, whereas that of methanol is about 80%. This suggests that methanol is a more efficient feedstock for producing hydrocarbons than glucose with the current catalyst at these reaction conditions.
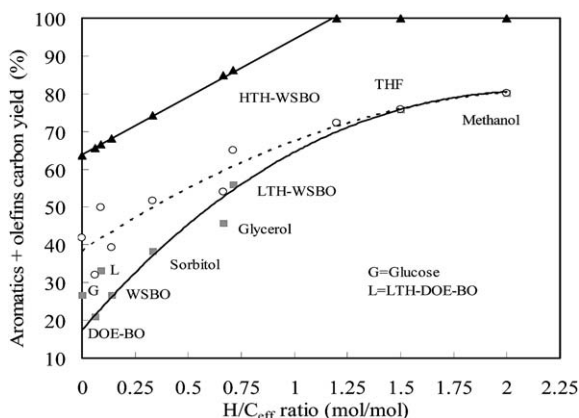

Fig. 6 The aromatic + olefin carbon yield for catalytic conversion of various biomass-derived feedstocks as a function of the hydrogen to carbon effective (H/C_{eff}) ratio. The H/C_{eff} ratios of the feedstocks: glucose, 0; DOE-BO, 0.06; LTH-DOE-BO, 0.09; WSBO, 0.14; sorbitol, 0.33; glycerol, 0.66; LTH-WSBO, 0.71; HTH-WSBO, 1.2; THF, 1.5 and methanol, 2. (▲ Theoretical carbon yield; ■ experimental carbon yield; ○ experimental/theoretical yield.)

Compared with DOE-BO, the aromatic + olefin yield of LTH-BO increases from 21% to 33%. The low temperature hydrogenation process resulted in an increase of the H/C_{eff} ratio of the bio-oil from 0.06 to 0.09. This process only used a small amount of hydrogen but resulted in a large increase in the yield of usable petrochemicals. This is probably because the hydrogenation step was able to stabilize the most unstable compounds in the bio-oil, which tends to form homogeneous coke when heated as shown in Table 2. The most unstable compounds formed coke on the catalyst surface during the hydrogenation step and thus the LTH-DOE-BO contains less thermally unstable molecules than DOE-BO (14% *vs.* 19%). These unstable molecules that tend to form homogeneous coke include aldehydes, ketones and furan derived oxygenates which contain unsaturated bonds.

In a separate reaction, we have previously converted furan (H/C_{eff} ratio = 0.5) under similar reaction conditions but short time on stream (5 min).[42] The catalyst deactivated rapidly within 5 min time on stream with a coke yield of 33% carbon. Tetrahydrofuran (THF) is the saturated form of furan. However, catalytic conversion of THF only produced 6% coke (see Fig. 8). This indicates that catalytic conversion of unsaturated compounds like furan produces large amounts of coke which rapidly deactivates the zeolite.

Low temperature hydrogenation of WSBO increased the H/C_{eff} ratio from 0.14 (WSBO) to 0.71 (LTH-WSBO). The aromatic + olefin yield improved from 27% to 56%. However, the LTH-WSBO still contains some hydrogen deficient compounds such as acetic acid (H/C_{eff} ratio = 0), levoglucosan (H/C_{eff} ratio = 0) and sorbitol (H/C_{eff} ratio = 0.33) (Table 1). These molecules need to be upgraded into hydrogen-rich molecules to further increase the petrochemicals yield. Hence we subjected LTH-WSBO to high temperature hydrogenation and converted it into high temperature hydrogenated WSBO (HTH-WSBO). With the H/C_{eff} ratio of HTH-WSBO increasing to 1.2, the aromatic + olefin yield increases to 72%. These results disclose that we can enhance the hydrocarbon yield by increasing the H/C_{eff} ratio of the feed. This is consistent with the results obtained by Gayubo *et al.*[64] who increased the hydrocarbon yield dramatically by co-conversion of bio-oil with methanol.

The product yields as a function of the H/C_{eff} ratio are shown in Fig. 7 and 8. As shown in Fig. 7(a), the aromatic and olefin yields increase from 12% and 15% to 24% and 56% with increasing H/C_{eff} ratio, respectively. For all feedstocks, the olefin yield is higher than the aromatic yield, and the gap increases with an increase of the H/C_{eff} ratio. If liquid hydrocarbons are the desired product then these olefins must be recycled or oligomerized.[42] The reaction temperature is high (600 °C) which favors the production of olefins.

The CO and CO_2 yields go through a maximum with respect to the H/C_{eff} ratio (Fig. 7(b)). CO was most likely produced by decarbonylation. Feedstocks with low H/C_{eff} ratio should make more CO because they are hydrogen-deficient compounds, which limits oxygen transferring into water and favors CO production. As shown in Fig. 7(b), sorbitol (H/C_{eff} ratio = 0.33) gave 28% CO yield which is more than that of glycerol (H/C_{eff} ratio = 0.66) which gave 22% CO yield. However, glucose, DOE-BO, LTH-DOE-BO and WSBO which have lower H/C_{eff} ratio than sorbitol produced less CO. This can be explained by homogeneous coke formation reactions where a large part of these feedstocks was
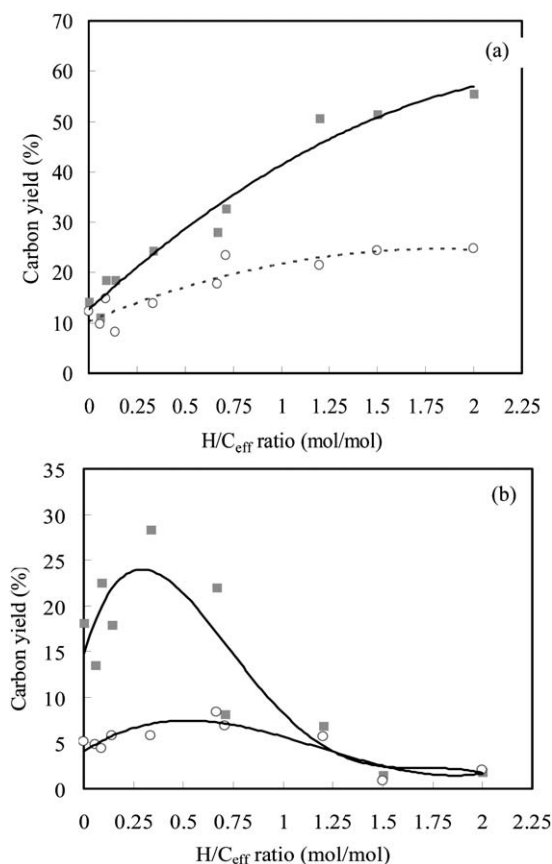
2304 | *Energy Environ. Sci.*, 2011, **4**, 2297–2307

This journal is © The Royal Society of Chemistry 2011

Fig. 7 Product carbon yields of catalytic conversion of various biomass-derived feedstocks as a function of the hydrogen to carbon effective (H/C_{eff}) ratio. (a) Olefin and aromatic yields (■ olefins; ○ aromatics); (b) CO and CO_2 carbon yields (■ CO; ○ CO_2). The H/C_{eff} ratios of the feedstocks: glucose, 0; DOE-BO, 0.06; LTH-DOE-BO, 0.09; WSBO, 0.14; sorbitol, 0.33; glycerol, 0.66; LTH-WSBO, 0.71; HTH-WSBO, 1.2; THF, 1.5 and methanol, 2.
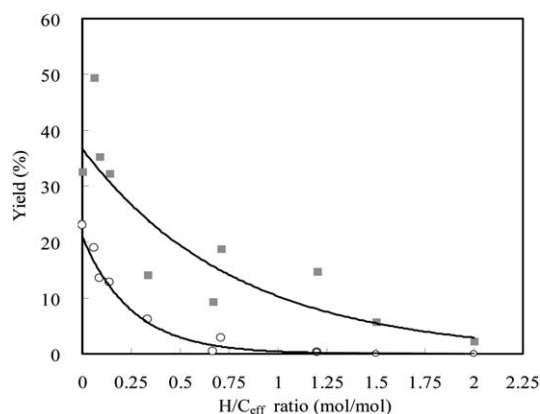
Fig. 8 Coke carbon yield (based on the total carbon of the feed) of catalytic conversion obtained from flow reactor and coke yield (based on the mass of the feed) of that obtained from TGA as a function of the hydrogen to carbon effective (H/C_{eff}) ratio of the feed. The H/C_{eff} ratios of the feedstocks: glucose, 0; DOE-BO, 0.06; LTH-DOE-BO, 0.09; WSBO, 0.14; sorbitol, 0.33; glycerol, 0.67; LTH-WSBO, 0.71; HTH-WSBO, 1.2; THF, 1.5 and methanol, 2. (■ Catalytic coke carbon yield; ○ homogeneous coke yield.)

converted into homogeneous coke before catalytic cracking with the catalyst. We conducted some blank experiments for homogeneous coke formation in the reactor. The experiments were operated at typical conditions as catalytic conversion run but without a catalyst. 45% carbon in the feed was converted into coke for WSBO, whereas only 5% carbon was converted into CO. However, catalytic conversion of WSBO gave about 18% carbon yield of CO. This indicates that CO is mainly produced in the catalytic process. Since CO_2 is mainly produced by water–gas shift reaction,[9] its yield as a function of the H/C_{eff} ratio has the same trend with that of CO. For bio-oil derived feedstocks, CO_2 can also be produced by decarboxylation reaction of acetic acid.

It should be noted that the coke obtained from catalytic conversion in the flow reactor is a total coke which includes homogeneous coke (defined as coke deposited on the reactor) and heterogeneous cokes (defined as coke deposited on the catalyst). In order to distinguish these two types of coke, the TGA experiments were conducted without catalyst to only obtain homogeneous coke. Fig. 8 shows the catalytic coke yield (based on the total carbon of the feed) and the non-catalytic coke yield (based on the mass of feedstock) as a function of the H/C_{eff} ratio. Both catalytic coke and non-catalytic coke yields decrease with increasing H/C_{eff} ratio. This decrease is greatest at H/C_{eff} ratios less than 0.25. The coke yield reaches a stable value at higher H/C_{eff} ratios. Compared with their H/C_{eff} ratio, catalytic cracking of the bio-oil derived feedstocks (including DOE-BO, LTH-DOE-BO, WSBO, LTH-WSBO and HTH-WSBO) produced more total coke due to a lot of homogeneous coke formation.

4.2. Deactivation rate of the catalyst as a function of hydrogen to carbon effective (H/C_{eff}) ratio

The rate of catalyst deactivation as defined in eqn (6) is introduced to describe the deactivation of the catalyst during the catalytic conversion process of biomass-derived feedstocks. The catalyst deactivation rates for catalytic conversion of different
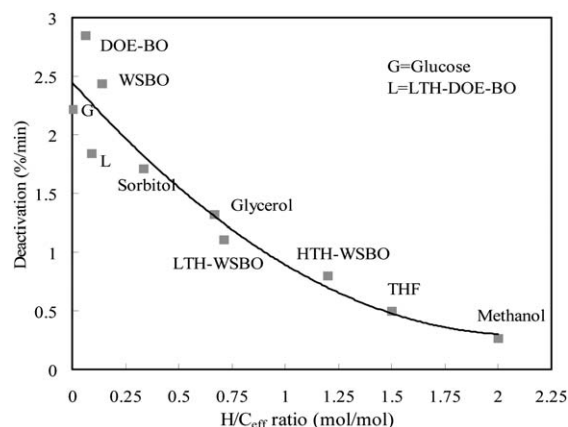

Fig. 9 The catalyst deactivation rates for catalytic conversion of different biomass-derived feedstocks as a function of hydrogen to carbon effective (H/C_{eff}) ratio. The H/C_{eff} ratios of the feedstocks: glucose, 0; DOE-BO, 0.06; LTH-DOE-BO, 0.09; WSBO, 0.14; sorbitol, 0.33; glycerol, 0.66; LTH-WSBO, 0.71; HTH-WSBO, 1.2; THF, 1.5 and methanol, 2.

biomass-derived feedstocks as a function of the H/C_{eff} ratio are shown in Fig. 9. As shown in the figure, the deactivation rate decreases with increasing H/C_{eff} ratio. Similar to coke carbon yield, the deactivation rate curve also decreases rapidly at low H/C_{eff} ratio and becomes stable at high H/C_{eff} ratio. This result indicates that the increase of the H/C_{eff} ratio of feedstocks can increase the stability of the catalyst due to low coke accumulation on the catalyst.

5. Conclusions

The general conclusion of this study is that the hydrogen to carbon effective (H/C_{eff}) ratio of biomass-derived feedstock can be used to estimate the overall olefin and aromatic yield, the coke yield, and the catalyst deactivation rate for the catalytic conversion of a range of biomass feedstocks using zeolite based catalysts. The aromatic + olefin carbon yield increases with increasing H/C_{eff} ratio. Lower H/C_{eff} ratio feedstocks produced more coke which rapidly deactivates the zeolite catalyst. Coke was produced from both homogeneous and heterogeneous reactions. TGA was done to determine the homogeneous coke yield. The result shows the formation of coke from homogeneous reactions decreases with increasing H/C_{eff} ratio. This can be used to guide the catalytic conversion of biomass and its derivatives into high yields of olefins and aromatics. Hydrogen deficient biomass feedstocks can be hydrogenated to increase their H/C_{eff} ratio before reaction with zeolite catalysts. The optimal amount of hydrogen to add to the biomass-derived feedstock for aromatic and olefin production is around a H/C_{eff} ratio of 1.2.

Acknowledgements

References

1 G. W. Huber, S. Iborra and A. Corma, *Chem. Rev.*, 2006, **106**, 4044–4098.
2 E. L. Kunkes, D. A. Simonetti, R. M. West, J. C. Serrano-Ruiz, C. A. Gartner and J. A. Dumesic, *Science*, 2008, **322**, 417–421.
3 S. T. Sie, *Stud. Surf. Sci. Catal.*, 1994, **85**, 587–631.
4 T. F. Degnan, *Top. Catal.*, 2000, **13**, 349–356.
5 A. Corma, M. Diaz-Cabanas, J. Martinez-Triguero, F. Rey and J. Rius, *Nature*, 2002, **418**, 514–517.
6 C. Marcilly, *J. Catal.*, 2003, **216**, 47–62.
7 A. V. Bridgwater, *Catal. Today*, 1996, **29**, 285–295.
8 S. Czernik and A. V. Bridgwater, *Energy Fuels*, 2004, **18**, 590–598.
9 A. Corma, G. W. Huber, L. Sauvanaud and P. O'Connor, *J. Catal.*, 2007, **247**, 307–327.
10 M. Stocker, *Angew. Chem., Int. Ed.*, 2008, **47**, 9200–9211.
11 Y. C. Lin and G. W. Huber, *Energy Environ. Sci.*, 2009, **2**, 68–80.
12 J. Q. Bond, D. M. Alonso, D. Wang, R. M. West and J. A. Dumesic, *Science*, 2010, **327**, 1110–1114.
13 S. Yaman, *Energy Convers. Manage.*, 2004, **45**, 651–671.
14 A. Demirbas, *Energy Sources, Part A: Recovery, Util. Environ. Eff.*, 2007, **29**, 753–760.
15 P. Gallezot, *ChemSusChem*, 2008, **1**, 734–737.
16 M. Olazar, R. Aguado, J. Bilbao and A. Barona, *AIChE J.*, 2000, **46**, 1025–1033.
17 L. H. Dao, M. Haniff, A. Houle and D. Lamothe, *ACS Symp. Ser.*, 1988, **376**, 328–341.
18 H. Chiang and A. Bhan, *J. Catal.*, 2010, **271**, 251–261.
19 A. Ausavasukhi, T. Sooknoi and D. E. Resasco, *J. Catal.*, 2009, **268**, 68–78.
20 A. Aho, N. Kumar, K. Eranen, T. Salmi, M. Hupa and D. Y. Murzin, *Fuel*, 2008, **87**, 2493–2501.
21 T. Danuthai, S. Jongpatiwut, T. Rirksomboon, S. Osuwan and D. E. Resasco, *Appl. Catal., A*, 2009, **361**, 99–105.
22 T. Q. Hoang, X. L. Zhu, T. Danuthai, L. L. Lobban, D. E. Resasco and R. G. Mallinson, *Energy Fuels*, 2010, **24**, 3804–3809.
23 F. A. Agblevor, O. Mante, N. Abdoulmoumine and R. McClung, *Energy Fuels*, 2010, **24**, 4087–4089.
24 F. A. Agblevor, S. Beis, O. Mante and N. Abdoulmoumine, *Ind. Eng. Chem. Res.*, 2010, **49**, 3533–3538.
25 F. Ates, A. E. Putun and E. Putun, *Energy Convers. Manage.*, 2005, **46**, 421–432.
26 F. Ates, A. E. Putun and E. Putun, *Fuel*, 2006, **85**, 1851–1859.
27 E. Putun, B. B. Uzun and A. E. Putun, *Biomass Bioenergy*, 2006, **30**, 592–598.
28 E. Putun, B. B. Uzun and A. E. Putun, *Energy Fuels*, 2009, **23**, 2248–2258.
29 P. Wang, S. H. Zhan, H. B. Yu, X. F. Xue and N. Hong, *Bioresour. Technol.*, 2010, **101**, 3236–3241.
30 A. Pattiya, J. O. Titiloye and A. V. Bridgwater, *J. Anal. Appl. Pyrolysis*, 2008, **81**, 72–79.
31 R. French and S. Czernik, *Fuel Process. Technol.*, 2010, **91**, 25–32.
32 H. Y. Zhang, R. Xiao, H. Huang and G. Xiao, *Bioresour. Technol.*, 2009, **100**, 1428–1434.
33 H. Y. Zhang, R. Xiao, D. H. Wang, Z. P. Zhong, M. Song, Q. W. Pan and G. Y. He, *Energy Fuels*, 2009, **23**, 6199–6206.
34 J. H. Jae, G. A. Tompsett, Y. C. Lin, T. R. Carlson, J. C. Shen, T. Y. Zhang, B. Yang, C. E. Wyman, W. C. Conner and G. W. Huber, *Energy Environ. Sci.*, 2010, **3**, 358–365.
35 C. A. Mullen and A. A. Boateng, *Fuel Process. Technol.*, 2010, **91**, 1446–1458.
36 N. Miskolczi, F. Buyong, A. Angyal, P. T. Williams and L. Bartha, *Bioresour. Technol.*, 2010, **101**, 8881–8890.
37 K. Giannakopoulou, M. Lukas, A. Vasiliev, C. Brunner and H. Schnitzer, *Bioresour. Technol.*, 2010, **101**, 3209–3219.
38 A. A. Lappas, M. C. Samolada, D. K. Iatridis, S. S. Voutetakis and I. A. Vasalos, *Fuel*, 2002, **81**, 2087–2095.
39 A. G. Gayubo, A. T. Aguayo, A. Atutxa, R. Aguado and J. Bilbao, *Ind. Eng. Chem. Res.*, 2004, **43**, 2610–2618.
40 A. G. Gayubo, A. T. Aguayo, A. Atutxa, R. Aguado, M. Olazar and J. Bilbao, *Ind. Eng. Chem. Res.*, 2004, **43**, 2619–2626.
41 B. Valle, A. G. Gayubo, A. T. Aguayo, M. Olazar and J. Bilbao, *Energy Fuels*, 2010, **24**, 2060–2070.
42 T. R. Carlson, Y. T. Cheng, J. H. Jae and G. W. Huber, *Energy Environ. Sci.*, 2011, **4**, 145–161.
43 T. R. Carlson, T. R. Vispute and G. W. Huber, *ChemSusChem*, 2008, **1**, 397–400.
44 J. Jae, G. A. Tompsett, A. J. Foster, K. D. Hammond, S. M. Auerbach, R. F. Lobo and G. W. Huber, *J. Catal.*, 2011, **279**, 257–268.
45 R. Rinaldi and F. Schuth, *Energy Environ. Sci.*, 2009, **2**, 610–626.
46 M. Hara, *Energy Environ. Sci.*, 2010, **3**, 601–607.
47 D. M. Alonso, J. Q. Bond and J. A. Dumesic, *Green Chem.*, 2010, **12**, 1493–1513.
48 P. L. Dhepe and A. Fukuoka, *ChemSusChem*, 2008, **1**, 969–975.

49 C. J. Serrano-Ruiz and J. A. Dumesic, *Energy Environ. Sci.*, 2011, **4**, 83–99.
50 C. Perego and D. Bianchi, *Chem. Eng. J.*, 2010, **161**, 314–322.
51 A. V. Bridgwater, *Appl. Catal., A*, 1994, **116**, 5–47.
52 N. Y. Chen, J. T. F. Degnan and L. R. Koenig, *Chem. Tech.*, 1986, **16**, 506.
53 I. M. Dahl and S. Kolboe, *J. Catal.*, 1994, **149**, 458–464.
54 I. M. Dahl and S. Kolboe, *J. Catal.*, 1996, **161**, 304–309.
55 M. Stocker, *Microporous Mesoporous Mater.*, 1999, **29**, 3–48.
56 M. Bjorgen, S. Svelle, F. Joensen, J. Nerlov, S. Kolboe, F. Bonino, L. Palumbo, S. Bordiga and U. Olsbye, *J. Catal.*, 2007, **249**, 195–207.
57 M. Bjorgen, S. Akyalcin, U. Olsbye, S. Benard, S. Kolboe and S. Svelle, *J. Catal.*, 2010, **275**, 170–180.
58 J. F. Haw, W. G. Song, D. M. Marcus and J. B. Nicholas, *Acc. Chem. Res.*, 2003, **36**, 317–326.
59 D. M. McCann, D. Lesthaeghe, P. W. Kletnieks, D. R. Guenther, M. J. Hayman, V. Van Speybroeck, M. Waroquier and J. F. Haw, *Angew. Chem., Int. Ed.*, 2008, **47**, 5179–5182.
60 T. P. Vispute, H. Y. Zhang, A. Sanna, R. Xiao and G. W. Huber, *Science*, 2010, **330**, 1222–1227.
61 A. T. Aguayo, A. G. Gayubo, M. Castilla, J. M. Arandes, M. Olazar and J. Bilbao, *Ind. Eng. Chem. Res.*, 2001, **40**, 6087–6098.
62 O. Mikkelsen and S. Kolboe, *Microporous Mesoporous Mater.*, 1999, **29**, 173–184.
63 M. Kaarsholm, B. Rafii, F. Joensen, R. Cenni, J. Chaouki and G. S. Patience, *Ind. Eng. Chem. Res.*, 2010, **49**, 29–38.
64 A. G. Gayubo, B. Valle, A. T. Aguayo, M. Olazar and J. Bilbao, *Ind. Eng. Chem. Res.*, 2010, **49**, 123–131.